doi:10.14311/ppt.2025.3.186
Plasma Physics and Technology **12**(3):186–189, 2025

BIDIRECTIONAL COUPLING OF JET PLUME AND PARTICLES IN A PLASMA SPRAYING PROCESS

T. Zhu*, M. M. Becker, M. Baeva

Leibniz Institute for Plasma Science and Technology, Felix-Hausdorff-Str. 2, 17489 Greifswald, Germany

* tao.zhu@inp-greifswald.de

Abstract. In previous studies of plasma spraying, a plasma jet was considered as a constant background in which particles are fed to be heated, molten and deposited on a target. This assumption is well justified for low feeding rates. At high rates, the particles can affect the plasma jet. This effect is studied here in terms of a bidirectional interaction between the plasma jet and the injected particles. The influence on the jet temperature and velocity in the plume, and the resulting coating is analysed.

Keywords: plasma spraying, modelling, plasma jet, particle tracing, bidirectional coupling.

1. Introduction

Atmospheric plasma spraying is a widely used technological process related to aerospace applications, formation and preparation of functional coatings. The end performance depends on individual components of the production chain: the properties of the generated plasma jet, and conditions in the jet plume, in which particles are fed and interact with the jet. Many works have been done on this topic over the years (see e.g., [1, 2] and the references therein). Simulation studies have been carried out in order to support the experimental studies and to provide a deeper insight into the physical processes. Some of the simulation studies employ two- or three-dimensional models [3, 4] with a single particle or multiple particle injection [3–6], unidirectional or bidirectional interaction of the plasma jet and the particles [3, 7]. The latter aspect gains importance at high particle feeding rate disturbing the plasma jet.

In previous works [8, 9], we carried out simulation studies and experiments of the commercial plasma torch Oerlikon Metco F4MB-XL with respect to the role of the plasma-cathode interaction, the influence of the fluid flow approach applied, and the understanding of the erosion of the cathode. These studies showed that the measured voltage and the thermal efficiency of the plasma torch agree well with the predicted values, provided that the electric power deposited in the cathode boundary layer and a fluid model including a high Mach number approach are taken into account. Furthermore, the removal of cathode material from the near-cathode region has been explained by a reversal of the electric field. In a more recent work [4], these studies have been extended to include the feeding of particles in the plume of the plasma jet. The heating of the particles appeared to occur as spatially fluctuating in a mixture of Ar and H_2 so that they can reach the substrate with a higher average temperature and velocity. In the latter study, the jet plume has been considered as pre-defined background, which is not influenced by the injected particles. This assumption was well justified for the feeding rates considered in these studies. Looking forward of increasing the process efficiency, higher feeding rates become of increasing interest. Therefore, the aim of the present work is to prove the appropriateness of the pre-defined plume conditions (referred to as the unidirectional approach below) for higher particle feeding rates. A bidirectional interaction of the plasma jet and the particles is implemented and its effect on the velocity and temperature of the jet plume and the layer deposition is studied.

2. Simulation workflow

The bidirectional modelling approach represents an extension of the model in [4], where an almost complete description was given. Note that main parts of this model included the solution of the fluid flow in the plume region (equations (14)–(18) in [4]) and description of the motion and heating of the injected particles (equations (1)–(10) in [4]). In what follows, a brief summary of the new features is provided. A schematic of the computational domain is shown in Figure 1, where half of the cylindrical domain with a diameter of 96 mm including the particle injector is shown. The injector tube has a diameter of 1.5 mm and is placed at a distance of 6 mm away from the torch nozzle and 10 mm away from the torch axis. The torch is operated in a mixture of Ar/H_2 (40/14 SLPM) at atmospheric pressure.

The main extension concerns modification of equations (14) and (18) in the basic model [4] in order to account for momentum and energy transfer from particles back to the plasma jet in the plume. The equations now read

$$\rho(\mathbf{u}\cdot\nabla)\mathbf{u} = \nabla\cdot[-p\mathbf{I}+\mathbf{K}] + \mathbf{F}_{\mathrm{bi}}, \tag{1}$$

$$\rho C_{\mathrm{pf}}\mathbf{u}\cdot\nabla T + \nabla\cdot\mathbf{q} = Q_{\mathrm{vd}} + Q_{\mathrm{p}} - Q_{\mathrm{rad}} + Q_{\mathrm{bi}}. \tag{2}$$

$$\frac{d(\mathbf{F}_{\mathrm{bi}})}{dt} = -\sum_{i=1}^{N}\frac{f_{\mathrm{rel},i}\cdot\mathbf{F}_{\mathrm{D},i}}{V_{\mathrm{mesh}}} \tag{3}$$

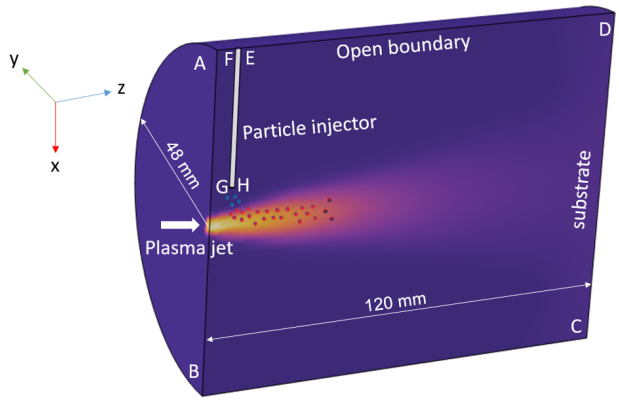

Figure 1. Schematic view of the computational domain.

$$\frac{d(Q_{\mathrm{bi}})}{dt} = -\sum_{i=1}^{N} \frac{f_{\mathrm{rel},i} \cdot Q_i}{V_{\mathrm{mesh}}} \tag{4}$$

The notations in equations (1) and (2) repeat those in the model in [4] except the last terms on the right hand sides. The term $\mathbf{F}_{\mathrm{bi}}$ in equation (1) represents the volume force that is equal in magnitude and opposite in direction to the total drag force that the fluid exerts on particles. For the sake of completeness, ρ is the mass density, $\mathbf{u}$ is the fluid velocity, p denotes the gas pressure, $\mathbf{I}$ is the identity matrix, $\mathbf{K}$ is the viscous stress tensor, C_{pf} is the heat capacity at constant pressure of the fluid, T is the gas temperature, $\mathbf{q}$ is the conductive heat flux, and the terms Q_{vd}, Q_{p}, and Q_{rad} are source terms accounting respectively for viscous dissipation, pressure work, and radiative losses. The time derivatives are defined in equation (3) and (4) to account for the behavior of a continuous stream of particles. The term $\mathbf{F}_{\mathrm{bi}}$ is obtained by performing a temporal integration over a sufficiently long interval to allow complete resolution of particle trajectories throughout the modeling domain. Here N is the total number of particles, $f_{\mathrm{rel},i}$ is the effective frequency of release, $\mathbf{F}_{\mathrm{D},i}$ is the drag force exerted on the i_{th} particle (see equation 2 in [4]), V_{mesh} is the mesh volume, where the sum is taken over the particles in the mesh element. The term Q_{bi} is the total heat loss of the fluid to heat the particle, which is calculated through equation (4) based on the same principle. As (3), Q_i is the heating power of i_{th} particle, which equals the term Q_{conv} in equation (8) in [4].

The simulation workflow is organized in an iterative way as follows. First, an initial solution of the plasma jet is obtained and the particle tracing is performed as for the case of unidirectional coupling [4]. The corresponding terms for the energy and momentum transfer with the surrounding gas are accumulated and recorded. As a second step, the terms $\mathbf{F}_{\mathrm{bi}}$ and Q_{bi} are included in equations (1) and (2) and the fluid flow part of the model and the particle tracing are re-solved. New values of $\mathbf{F}_{\mathrm{bi}}$ and Q_{bi} are obtained. The procedure is repeated until no changes in the terms are observed within a given accuracy ($\sim$1%). Usually, 3 to 5 iteration cycles are enough.

3. Results and discussion

The injected particles are made of Al_2O_3. A normal statistical distribution with a mean value of 100 µm and a standard deviation of 20 µm is adopted for the sampling of the particle size. The material properties of the particles are the same as in the previous work [4] but the particles themselves are now larger and therefore a phase change is not taken into account. A parametric study is carried out for mass flow rates of 0.5, 1.0, 2.0 and 4.0 g s^{-1} of the injected powder and injection velocities (v_0) of 1, 15, and 30 m s^{-1}. Note that the injection velocity is set equal to the average velocity of the carrier gas (v_{avg}). The mass flow rate determines how frequently particles are released. the results obtained are shown in Figures 2 to 4.

Figures 2 (a) and (b) show the isotherm of jet temperature and velocity contours at given injection velocity and mass flow rates. Due to bidirectional coupling, the energy used for particle heating is taken away from the jet plume at the same time. Therefore, the energy transfer naturally leads to temperature decrease in the jet plume, especially for the isotherms lower than 10 kK. With increasing feeding mass flow rate, the energy transfer and temperature decrease is enhanced. However, the isotherms 12 kK and 14 kK are hardly influenced due to small interaction between jet plume and particles. Similar influence is shown for the velocity contours in Figure 2(b). Momentum transfer between jet plume and particles slows down the jet plume in the core region. While at the vicinity of torch exit and substrate, the fluid velocity is kept close under various mass flow rates. This can be explained by less momentum exchange at the torch exit and no-slip boundary condition at the substrate. For more clearance, the distribution of the bidirectional coupling terms Q_{bi} and the z component of $\mathbf{F}_{\mathrm{bi}}$ are shown in Figures 3(a) and (b), respectively. The z component of $\mathbf{F}_{\mathrm{bi}}$ is presented here because momentum exchange in the z direction is more dominant compared with that of the radial direction. These terms are calculated synchronously with the particle tracing model at each time step along the particle trajectory, until all the particles reach the substrate.

Moreover, results of these terms at each time step are kept and accumulated over time so that it does not vanish with time and can be used as source terms for the jet model. One can see from Figure 3(a) and (b) that, the maximum absolute values of Q_{bi} and the z component of $\mathbf{F}_{\mathrm{bi}}$ are located at the region (-3<x<0 mm, 5<z<12 mm) of the jet plume and gradually fading along the trajectories. This means that the energy and momentum exchange is most intensive and concentrated in the upstream region of the jet plume and progressively diminishing. It is the presence of intensive and local exchange of energy and momentum that leads to a decrease in the fluid temperature and velocity in the whole calculation domain in Figure 2.

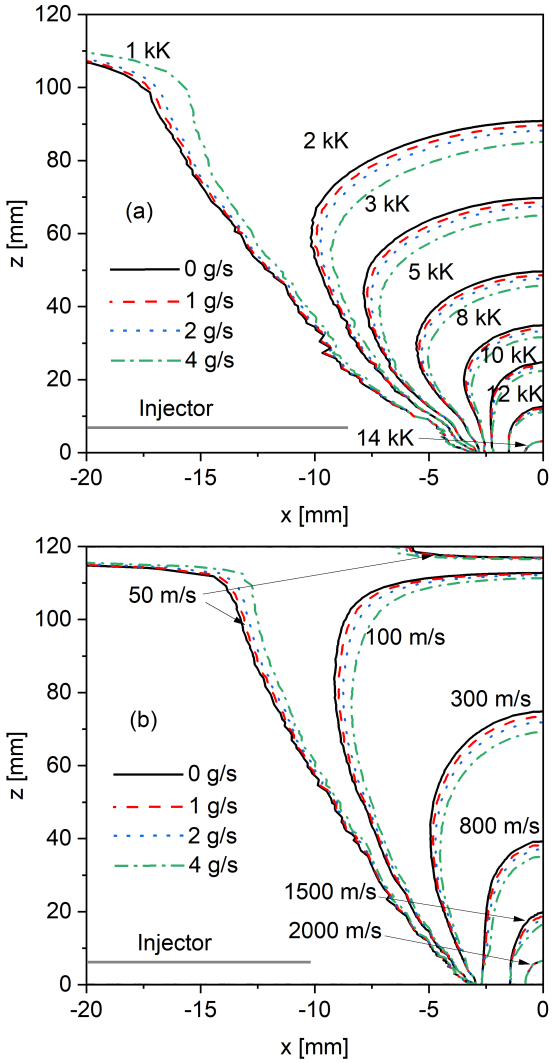

Figure 2. Temperature isotherm (a) and velocity contours (b) of the plasma jet plume at injection velocity of 30 $m\,s^{-1}$ and various mass flow rates.

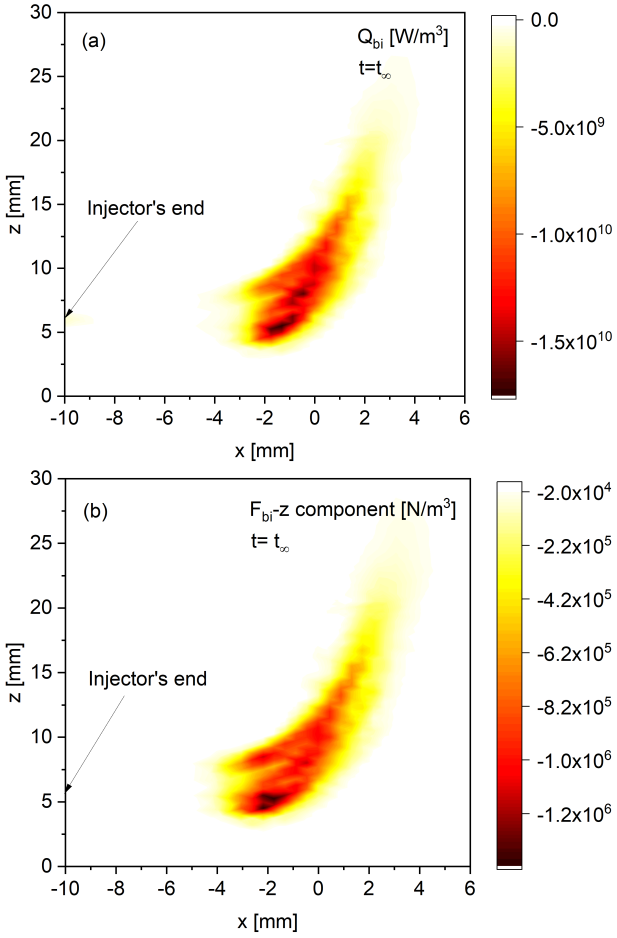

Figure 3. Distribution of Q_{bi} (a) and z component of $\mathbf{F}_{\mathrm{bi}}$ (b) at injection velocity of 30 $m\,s^{-1}$ and mass flow rate of 4 $g\,s^{-1}$. Both of the results are accumulated over time and reach a steady state.

The effect of the bidirectional interaction on the distribution of the particles on the substrate is considered next. Figure 4 shows the plane of the substrate xy for the case of injection velocity $v_0 = 15\,\mathrm{m\,s^{-1}}$ and $30\,\mathrm{m\,s^{-1}}$ under mass flow rate of $4\,\mathrm{g\,s^{-1}}$. Solid symbols indicate the positions of the arriving particles in the case of the unidirectional coupling of jet and particles, while the open symbols correspond to the bidirectional one. Note that in the unidirectional interaction the plasma jet is a pre-computed background without accounting for the mass flow rate of the injected particles. One can see that the main effect of bidirectional coupling is a minor shift of the particles, i.e., slightly deviated from the original position obtained from unidirectional coupling. The injection velocity has a dominant influence on the particle distribution at the substrate. A larger injection velocity provides the particles more momentum and penetrating the jet plume to form a fan-shaped area, while low injection velocity brings the majority of particles more concentrated in the region x<10/,mm. Furthermore, arriving metrics for results obtained with uni- and bidirectional coupling are respectively given in Table 1 to give a more quantitative analysis. An increase of 14.6% of particles arrived on the substrate is obtained under bidirectional coupling, but with lower average temperature and velocity. It is important to mention that without considering a phase change process, the estimated peak thickness cannot represent the real thickness of deposition on the substrate. However, these metrics reflect the slightly higher degree of particle concentration on the substrate in modeling results including bidirectional coupling.

4. Conclusions

The present work completes previous simulation studies related to plasma spraying, in which a precomputed distribution of the plasma jet properties without account for the effect of injected particles was considered. This previous approach includes a unidirectional coupling of the jet plume and the tracing of the injected particles. Since particles are heated and moved by the plasma jet, effects related to the conservation of momentum and energy of the plasma jet are expected to occur, e.g., deceleration and a

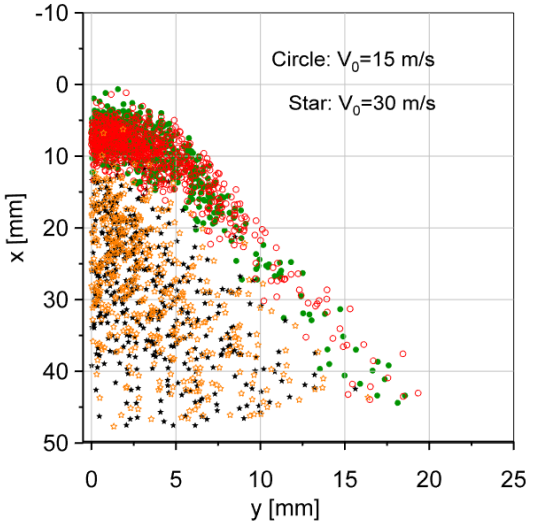

Figure 4. Positions of the particles arriving the substrate with given injection velocities and mass flow rates of 4 g s^{-1}. Solid symbols-filled in green and black-for unidirectional coupling, open symbols-without interior colors-for bidirectional coupling.

temperature decrease. In order to account for such effects, a bidirectional approach is considered here. The latter implies additional terms introduced into the equations for conservation of momentum and energy of the plasma jet. These terms are integrated over a sufficiently long interval to allow complete resolution of particle trajectories throughout the modeling domain. The coupling of plasma jet computation and the particle tracing appears here as bidirectional. Several computational cycles are needed in order to get a final solution. The results obtained can be summarized as follows.

Bidirectional coupling enables the energy and momentum exchange between particles and jet plume. The most intensive exchange of energy and momentum occurs at the upstream region, then progressively diminishing downstream. The bidirectional coupling leads to temperature and velocity decrease in the whole jet plume region compared to results neglecting bidirectional coupling. Nevertheless, the unidirectional simulation approach is capable of predicting the particles trajectories and their distribution on the substrate. Bidirectional simulation results in a slightly deviation of the particle impact on the substrate from the original position obtained from unidirectional coupling. The injection velocity is dominantly responsible for the distribution of particles on the substrate. Quantitative analysis of the influence of bidirectional coupling compared to unidirectional coupling demonstrated that the former slightly enhances particle deposition on the substrate and promotes a higher degree of concentration in their spatial distribution. Therefore, the main benefit of the bidirectional coupling can be seen as a global refinement of the jet properties with limited influence on the distribution of the particles arriving the substrate.

Arriving metrics	**Method 1**	**Method 2**
Arrived particles	402	461
Avg. temperature	893.9 K	830.5 K
Avg. velocity	115.5 m s^{-1}	97.5 m s^{-1}
Avg. flight time	1.38 ms	1.45 ms
Peak thickness	97.1 µm	113 µm

Table 1. Comparison of arriving metrics between two methods (Method 1: unidirectional coupling, Method 2: bidirectional coupling) under injection velocity of 30 m s^{-1} and particle feeding rate of 4 g s^{-1}.

References

[1] A. Vardelle, C. Moreau, N. Themelis, and C. Chazelas. A perspective on plasma spray technology. *Plasma Chem Plasma Process*, 35(3):491–509, 2015. doi:10.1007/s11090-014-9600-y.

[2] C. Chazelas, J. Trelles, and A. Vardelle. The main issues to address in modeling plasma spray torch. *J Therm Spray Technol*, 26(1-2):3–11, 2017. doi:10.1007/s11666-016-0500-y.

[3] K. Bobzin and M. Öte. Modeling plasma–particle interaction in multi-arc plasma spraying. *J Therm Spray Tech*, 26(3):279–291, 2017. doi:10.1007/s11090-022-10290-y.

[4] T. Zhu, M. Baeva, H. Testrich, et al. Effect of a spatially fluctuating heating of particles in a plasma spray process. *Plasma Chem Plasma Process*, 43(1):1–24, 2023. doi:10.1007/s11090-022-10290-y.

[5] R. Djebali, B. Pateyron, and M. ElGanaoui. Scrutiny of plasma spraying complexities with case study on the optimized conditions toward coating process control. *Case Studies in Thermal Engineering*, 6:171–181, 2015. doi:10.1016/j.csite.2015.09.005.

[6] R. Djebali, M. ElGanaoui, A. Jaouabi, and B. Pateyron. Scrutiny of spray jet and impact characteristics under dispersion effects of powder injection parameters in aps process. *International Journal of Thermal Sciences*, 100:229–239, 2016. doi:10.32604/fhmt.2025.063375.

[7] Z. Pan, X. Chen, X. Yuan, et al. The effects of graphite particles on arc plasma characteristics. *Plasma Chem Plasma Process*, 41(4):1183–1203, 2021. doi:10.32604/fhmt.2025.063375.

[8] M. Baeva, T. Zhu, T. Kewitz, et al. Self-consistent cathode-plasma coupling and role of the fluid flow approach in torch modeling. *J Therm Spray Tech*, 30:1737–1750, 2021. doi:10.1007/s11666-021-01261-4.

[9] M. Baeva, M. S. Benilov, T. Zhu, et al. Modelling and experimental evidence of the cathode erosion in a plasma spray torch. *J Phys D: Appl Phys*, 55:365202, 2022. doi:10.1088/1361-6463/ac791c.